International Journal of Nanomedicine Dovepress

Open Access Full Text Article ORIGINAL RESEARCH

Characterization and Performance Evaluation of Magnesium Chloride-Enriched Polyurethane Nanofiber Patches for Wound Dressings

Mohan Prasath Mani[1,2], Hemanth Ponnambalath Mohanadas[3], Ahmad Athif Mohd Faudzi[4,5], Ahmad Fauzi Ismail[6], Nick Tucker[7], Shahrol Mohamaddan[8], Manikandan Ayyar[9], Tamilselvam Palanisamy[1], Rajasekar Rathanasamy[10], Saravana Kumar Jaganathan[11–13]

[1]Department of Mechanical Engineering, SNS College of Technology, Coimbatore, TN, India; [2]School of Biomedical Engineering and Health Sciences, Faculty of Engineering, Universiti Teknologi Malaysia, Skudai, JB, Malaysia; [3]Device Development Group, New Product Research and Development, Abbott Diabetes Care, Alameda, CA, USA; [4]School of Electrical Engineering, Faculty of Engineering, UniversitiTeknologi Malaysia, Skudai, JB, Malaysia; [5]Centre for Artificial Intelligence and Robotics, Universiti Teknologi Malaysia, Kuala Lumpur, SG, Malaysia; [6]Advanced Membrane Technology Research Centre (AMTEC), School of Chemical and Energy Engineering, Universiti Teknologi Malaysia, Skudai, JB, Malaysia; [7]School of Engineering and Physical Sciences, College of Health and Sciences, University of Lincoln, Lincoln, LS, UK; [8]Innovative Global ProgramCollege of Engineering Shibaura Institute of Technology Tokyo, Tokyo, Japan; [9]Department of Chemistry, Centre for Materials Chemistry, Karapagam Acdemy of Higher Education, Coimbatore, TN, India; [10]Department of Mechanical Engineering, Kongu Engineering College, Perunduari, TN, India; [11]Institute of Research and Development, Duy Tan University, Da Nang, Vietnam; [12]School of Engineering & Technology, Duy Tan University, Da Nang, Vietnam; [13]Biomaterials and Tissue Engineering, School of Engineering and Physical Sciences, College of Health and Sciences, University of Lincoln, Lincoln, LS, UK

Correspondence: Saravana Kumar Jaganathan, Institute of Research and Development, Duy Tan University, Da Nang, Vietnam, Email jaganathansaravanakumar@dtu.edu.vn; sjaganathan@lincoln.ac.uk

Purpose: Wound patches are essential for wound healing, yet developing patches with enhanced mechanical and biological properties remains challenging. This study aimed to enhance the mechanical and biological properties of polyurethane (PU) by incorporating magnesium chloride ($MgCl_2$) into the patch.

Methodology: The composite patch was fabricated using the electrospinning technique, producing nanofibers from a mixture of PU and $MgCl_2$ solutions. The electrospun PU/$MgCl_2$ was then evaluated for various physico-chemical characteristics and biological properties to determine its suitability for wound healing applications.

Results: Tensile strength testing showed that the mechanical properties of the composite patch (10.98 ± 0.18) were significantly improved compared to pristine PU (6.66 ± 0.44). Field scanning electron microscopy (FESEM) revealed that the electrospun nanofiber patch had a smooth, randomly oriented non-woven structure (PU – 830 ± 145 nm and PU/$MgCl_2$ – 508 ± 151 nm). Fourier infrared spectroscopy (FTIR) confirmed magnesium chloride's presence in the polyurethane matrix via strong hydrogen bond formation. Blood compatibility studies using coagulation assays, including activated partial thromboplastin time (APTT), prothrombin time (PT), and hemolysis assays, demonstrated improved blood compatibility of the composite patch (APTT – 174 ± 0.5 s, PT – 91 ± 0.8s, and Hemolytic percentage – 1.78%) compared to pristine PU (APTT – 152 ± 1.2s, PT – 73 ± 1.7s, and Hemolytic percentage – 2.55%). Antimicrobial testing showed an enhanced zone of inhibition (Staphylococcus aureus – 21.5 ± 0.5 mm and Escherichia coli – 27.5 ± 2.5 mm) compared to the control, while cell viability assays confirmed the non-cytotoxic nature of the developed patches on fibroblast cells.

Conclusion: The study concludes that adding $MgCl_2$ to PU significantly improves the mechanical, biological, and biocompatibility properties of the patch. This composite patch shows potential for future wound healing applications, with further studies needed to validate its efficacy in-vivo.

Keywords: wound dressings, polyurethane, $MgCl_2$, biomaterial, nanofibers

Introduction

Skin damage can alter the skin functions to various extend, even leading to death.[1] Various factors, ranging from diabetes, burns, mechanical injuries to surgical interventions, can precipitate such damage.[2] While minor skin injuries

Received: 23 January 2024
Accepted: 19 July 2024
Published: 1 November 2024

often undergo natural repair processes, more severe wounds necessitate the use of skin substitutes to facilitate healing and regeneration.[2] In these critical situations, the efficacy of wound management heavily relies on the selection of optimal wound dressings. Ideal dressings should possess a combination of desirable properties: antimicrobial activity, biocompatibility, biodegradability, non-toxicity, adequate porosity, appropriate water vapor transmission rate to ensure a moist healing environment, robust mechanical strength, and permeability for gaseous exchange, which is essential for cell viability.[3] Recently, polymeric wound dressings gained a wide attention in wound healing applications.

Polyurethane (PU) is a highly versatile synthetic polymer that has garnered significant interest within the realm of wound healing applications due to its remarkable physicochemical attributes.[4] This polymer is composed of repeating units of isocyanates and polyols, which can be chemically modified to produce materials with diverse mechanical, thermal, and biodegradation properties, enabling the tailoring of PU materials for specific tissue engineering applications, including wound healing, nerve regeneration, and cartilage repair.[5] Additionally, PU exhibits biocompatibility, making it an attractive candidate for medical implants and tissue scaffolds.[6] The versatility of PU is further highlighted by its ability to be processed into diverse morphologies, including films, fibers, and foams, and its capacity to incorporate biologically active molecules, such as growth factors and drugs.[7] In the context of wound dressing applications, PU patches have demonstrated remarkable efficacy in providing antimicrobial activity and promoting cell growth and differentiation.[8]

Recently scaffolds containing metallic particles have gained huge potential in wound healing applications.[9,10] Magnesium ions have garnered increasing attention in the field of regenerative medicine due to its unique biological and mechanical properties. Magnesium ions have been shown to promote cell proliferation, activate signaling pathways, cofactor activation, and modulate gene expression,[11,12] making them a promising candidate for wound dressing applications. In addition, Mg ions has a low toxicity and high biocompatibility, making it an attractive option for biomedical applications.[12]

Manufacturing techniques is emerging as a crucial adjunctive tool in medicine, especially with its applications in healthcare including anatomical personalization for prostheses, orthoses, and splints, manufacturing biomedical implants, wound healing applications, and bio-composite structures.[13] The wound dressing patches can be fabricated through several manufacturing techniques such as self-assembly, phase separation, freeze drying, drawing and electrospinning.[14] In our study, the electrospinning technique is used to create patch for wound healing applications. Electrospinning is a highly regarded scaffold technique within the field of regenerative medicine due to its ability to produce nanofiber patch that closely mimic the extracellular matrix (ECM) structure of the tissue.[15] The small diameters of the electrospun nanofibers provide a substantial surface area for cell attachment, which enhances tissue growth and development.[16] Additionally, the electrospinning process enables the creation of patch with controlled pore sizes, which optimizes the exchange of nutrients and waste products, as well as adjusting mechanical strength.[17]

Building upon previous studies that investigated the incorporation of $MgCl_2$ into poly (vinyl alcohol) (PVA) and polycaprolactone (PCL) composites, this research pioneers a novel application in wound healing. While earlier research focused on the enhancement of mechanical properties[18] and hydrophilicity of scaffolds for bone regeneration,[19] this study marks the first exploration of $MgCl_2$ and polyurethane in a single-step electrospinning process for wound healing applications. In this study, we hypothesized that utilizing a combination of polyurethane (PU) and $MgCl_2$ in the electrospinning process for wound healing applications would result in improved mechanical and biocompatibility properties. Our experiments and analysis aimed to advance the research in wound dressings and offer valuable insights into the potential of using polyurethane and $MgCl_2$ in the electrospinning process as a material for wound healing applications.

Materials and Methodology

Materials

The study utilized Tecoflex EG 80A polyurethane which was provided by Lubrizol (USA). It contains 35% of hard segments (Shore A hardness= 72, specific gravity= 1.04) with a melting point of soft segment at 22°C. Its constituent formulation contains hard segment of methylene bis (cyclohexyl) diisocyanate (hydrogenated MDI, H12MDI), the soft

segment of polytetramethylene oxide with molecular weight= 1000 g/mol and 1.4 butane diol as a chain extender. Magnesium chloride hexahydrate was purchased from Sigma Aldrich. Dimethylformamide (DMF) was purchased from Merck (USA), and the anticoagulant reagents used in the blood compatibility studies were obtained from Thermo Fisher Scientific (Selangor, Malaysia).

Preparation of Solutions

The PU (9 wt%) and $MgCl_2$ (4 wt%) solutions were prepared by dissolving the materials in DMF. To fabricate the composite patch, the PU and $MgCl_2$ solutions were mixed in a ratio of 7:2 (w/v%) respectively. The ratio was chosen based on preliminary studies, which showed that this combination resulted in the beadle's formation of fibers from polyurethane.

Fabrication of Wound Patch

The composite solution of PU and $MgCl_2$ was converted into nanofibers using electrospinning. This process involves the application of a high voltage to the solution, which causes it to be expelled from a needle tip and deposited onto a collector in the form of nanofibers. The parameters for the electrospinning process were carefully controlled to ensure the production of uniform and high-quality nanofibers. The solution was fed at a rate of 0.2 mL/h, with an applied voltage of 10.5 kV and a collector distance of 20 cm.

Characterizations Studies

Characterization studies play a crucial role in determining the suitability of a material for wound dressing applications. These studies provide information about the physicochemical and morphological features of the patches, which can impact cell behavior and tissue growth.

FESEM

The FESEM images of the developed nanofibers were obtained using a Field Emission Scanning Electron Microscope (FESEM, Hitachi SU8020, Tokyo, Japan) unit. The samples, which had a gold layer, were scanned at multiple locations to ensure comprehensive analysis. The images were then examined at higher magnification to observe the structural details of the nanofibers. To determine the average diameter of the nanofibers, 30 randomly selected locations were measured, and the results were used to calculate the mean diameter of the fibers.

FTIR

The IR data of the developed fibers was obtained using Attenuated Total Reflectance Fourier Transform Infrared (ATR FTIR, Thermo Fischer Scientific, Waltham, MA, USA) spectroscopy equipment. The absorbance mode was used to study the IR spectra of the nanofibers, and the spectra were recorded over a range of 600–4000 cm^{-1}. This technique allowed for the analysis of the functional groups present in the fibers and provided insights into their chemical composition.

Uniaxial Mechanical Testing

The uniaxial tensile strength of the developed nanofibers was evaluated using a Gotech Testing Machines, AI-3000. A sample with dimensions of 40 mm x 10 mm was placed in the grips of the tensile equipment and the test was performed at a crosshead rate of 10 mm/min. The average strength was calculated from the stress-strain curves obtained during the test.

Thermal Analysis

The thermal behavior of the developed nanofibers was studied using a Perkin Elmer Thermal Gravimetric Analysis (TGA, PerkinElmer, Waltham, MA, USA) unit. The experiment was conducted in a nitrogen atmosphere with a heating rate of 10°C/min and a temperature range of 30 to 1000°C.

Atomic Force Microscopy (AFM)

The surface roughness of the patch was characterized using an Atomic Force Microscope (AFM, NanoWizard®, JPK Instruments, Berlin, Germany) unit. The AFM patterns were captured by scanning a 20 μm x 20 μm area with a pixel resolution of 512×512.

Contact Angle Measurement

Static contact angle measurements were conducted using Video Contact angle (VCA) equipment (AST products, Inc., Billerica, MA, USA). A 0.5 μL water droplet was placed on the membrane, and a high-speed video camera was used to record a static image of the droplet within 20 seconds. The results were reported as an average of at least three separate recordings for each type of sample.

Blood Compatibility Analysis

Blood compatibility analysis is an important aspect of evaluating the suitability of a material for biomedical applications, including tissue engineering. It is performed to assess the interactions between the material and blood components and to determine the risk of adverse events, such as thrombosis, embolism, and inflammation. The results of these tests provide important information about the blood compatibility of the material, which is critical in determining its suitability for use in wound dressing applications. Experimental procedures involving the handling of blood were approved by the Ethics committee, Faculty of Biosciences and Medical Engineering, Universiti Teknologi Malaysia, with reference number UTM.J.45.01/25.10/3Jld.2(3). Written informed consent was obtained from all blood donors prior to their participation in the study.

APTT and PT Analysis

The APTT test is a laboratory test used to evaluate the intrinsic pathway of coagulation, which is one of the two main pathways involved in blood clotting. This test measures the time it takes for the formation of a blood clot in a plasma sample that has been activated with partial thromboplastin, a reagent made from animal tissue. The APTT assay was performed by incubating the nanofiber mats with 50 μL of platelet-poor plasma (PPP) at 37°C followed by the addition of 50 μL of rabbit brain cephaloplastin reagent for 3 minutes at 37°C followed by adding 50 μL calcium chloride. The time taken for a blood clot to form was recorded as the APTT time.[20,21]

The PT test is a laboratory test used to evaluate the extrinsic pathway of coagulation, which is one of the two main pathways involved in blood clotting. This test measures the time it takes for the formation of a blood clot in a plasma sample that has been activated with thromboplastin, a reagent made from animal tissue. Similarly, to APTT test, the PT time was measured by incubating the nanofiber mats with 50 μL of PPP followed by the addition of 50 μL of NaCl-thromboplastin reagent (Factor III). The time taken for a blood clot to form was recorded as the PT time.[20,21]

Hemolysis Percentage

The biocompatibility of the fabricated nanofibers was evaluated through an assay to measure their hemolytic activity. A piece of the nanofibers was incubated with diluted blood and saline solution at 37°C for duration of 1 hour. The negative control group was comprised of the diluted blood and saline solution, while the positive control group was composed of diluted blood and distilled water. Subsequently, the samples underwent centrifugation for 15 minutes at 3000 revolutions per minute (RPM) to separate the supernatant from any cellular debris. The supernatant was then analyzed for absorbance using ultraviolet spectrophotometry, with a wavelength of 542 nm. The positive control absorbance was set to 100% and the absorbance of each sample was expressed as the percentage of hemolysis relative to the positive control.[20,21]

Antimicrobial Testing

Antimicrobial activity of developed electrospun membranes was tested in Staphylococcus aureus and Escherichia coli. The bacteria were grown in Mueller Hinton Agar (MHA) incubated at 20°C. About 15 mL of MHA medium was poured

into sterile petriplates and the plates were allowed to solidify for 5 minutes. After, the wells with 6 mm diameter were prepared and the prepared samples were placed with different concentrations (50 ug/mL, 100 ug/mL, 250 ug/mL, and 500 ug/mL) and incubated at 37°C for 24 h. By measuring the diameter of the inhibitory zones (mm) surrounding the wells, antibacterial activity was assessed.

Cell Viability Analysis

Primary skin dermal cells, known as HDF (Human Skin Fibroblast Cells 1184, ECACC, UK), were grown in Dulbecco's Modified Eagle Medium (DMEM) media with 10% fetal bovine serum and kept at 37°C with 5% CO_2. Three days a week, the media was changed. After being cut into size of 0.5 cm × 0.5 cm, the electrospun membranes were inserted onto the 96 well plates. The cells were seeded into the membranes at a density of 10×10^3 cells/cm^2 once they had reached 80% confluence. After five days of incubation, the cell viability was assessed using the MTT test. Following five days of culture, 3-(4,5-Dimethylthiazol-2-yl)-2,5-Diphenyltetrazolium Bromide (MTT) solution was added to the medium and the mixture was then incubated for four hours. A spectrophotometric plate reader was used to detect the absorbance at a wavelength of 490 nm after 4 hours.[22]

Statistical Analysis

One way analysis of variance (ANOVA) was conducted followed by Dunnett post hoc test to analyze the statistical significance ($p < 0.05$). All tests were performed thrice and the analyzed data were expressed as mean ± SD for three trials. A representative of three images was presented for qualitative experiments.

Results and Discussion

FESEM Investigation

Figure 1 displays the FESEM images of the fabricated electrospun nanofiber mats. The electro spun nanofiber patch presents a smooth and randomly oriented non-woven structure. The average fiber diameter of pristine polyurethane (PU) was found to be 830 ± 145 nm, while the PU/magnesium chloride ($MgCl_2$) composite exhibited a fiber diameter of 508 ± 151 nm ($p < 0.05$). Furthermore, to elucidate the distribution of $MgCl_2$ within the polyurethane matrix, we conducted an Energy Dispersive X-ray Spectroscopy (EDS) analysis. The obtained results, depicted in Figure 2, confirm the presence of magnesium (1%) in the polyurethane matrix, in addition to the carbon and oxygen content observed in the PU/MgCl2 samples during the FESEM analysis.

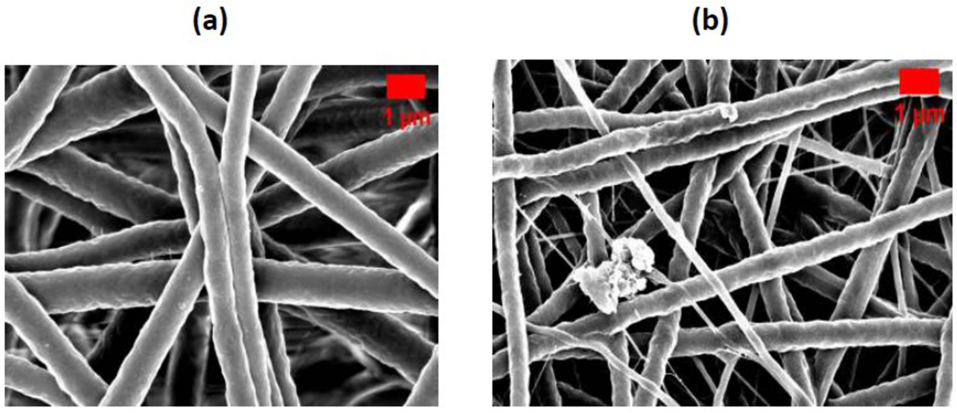

Figure 1 The SEM images of (**a**) PU and (**b**) PU/$MgCl_2$ patch.

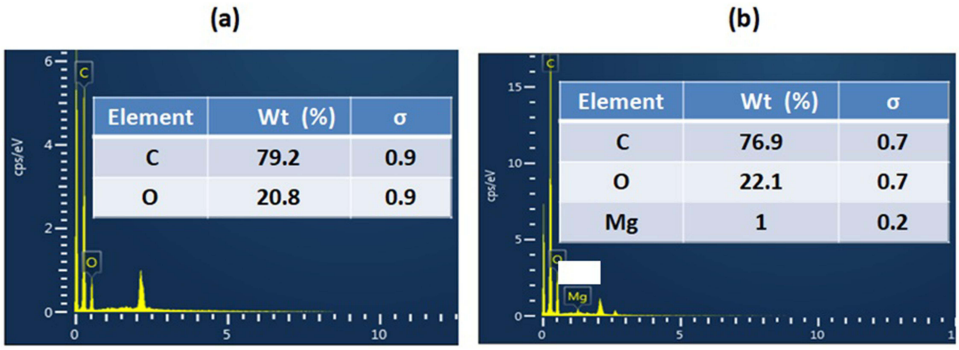

Figure 2 EDX spectra of the developed electrospun (**a**) PU and (**b**) PU/$MgCl_2$ patch.

FTIR Analysis

The FTIR spectra were used to determine the chemical composition of the electrospun nanofibers and details are shown in Figure 3. The FTIR spectra of the prisitne PU showed several peaks including those corresponding to the NH group (3318 cm^{-1}), CH group (2920 cm^{-1} and 2852 cm^{-1}), CO group (1730 cm^{-1} and 1701 cm^{-1}), and NH and CH vibrations (1531 cm^{-1} and 1597 cm^{-1} and 1414 cm^{-1}, respectively). The peaks at 1221 cm^{-1}, 1105 cm^{-1}, and 770 cm^{-1} correspond to the CO group with respect to alcohol.[22]

When $MgCl_2$ was added to the PU, no new peaks were observed in the FTIR spectra of the nanocomposite membranes. However, the intensity of the PU peaks increased, indicating strong hydrogen bond formation between the PU molecules and $MgCl_2$.[23] This is illustrated in Figure 4. Further, the shift of the CH peak from 2920 cm^{-1} to 2940 cm^{-1} was observed on adding $MgCl_2$ to the polyurethane matrix.[24]

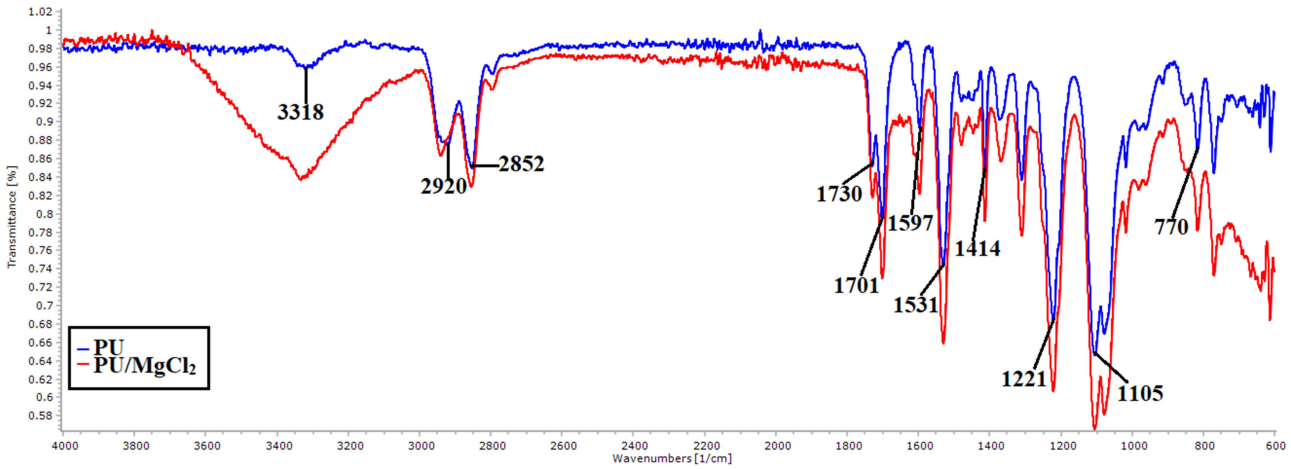

Figure 3 FTIR images of electrospun PU and PU/$MgCl_2$ patch.

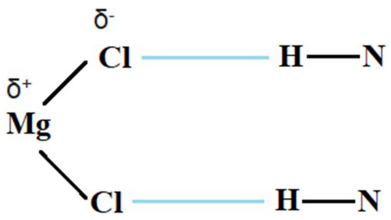

Figure 4 Interaction of $MgCl_2$ with the amide group of polyurethane at the region 3318 cm^{-1}.

Wettability Measurements

The results of the wettability measurements show that the addition of $MgCl_2$ to polyurethane improved its wettability. The pristine PU nanofibrous membrane had a contact angle of 109° ± 1°, which is hydrophobic. However, with the addition of $MgCl_2$, the contact angle was decreased to 78 ± 2°, indicating hydrophilic behavior ($p < 0.05$).

TGA Analysis

TGA was conducted to evaluate the thermal stability of electrospun PU and PU/ $MgCl_2$ nanocomposites. Figure 5 shows the TGA curves of electrospun PU and PU/ $MgCl_2$. The results showed that the addition of $MgCl_2$ decreased the initial degradation temperature from 284°C in pristine PU to 198°C in PU/ $MgCl_2$. The Differential Thermogravimetric Analysis (DTG) analysis (Figure 6) revealed that the number of weight loss peaks in PU increased from three to four with the addition of $MgCl_2$. Additionally, it was evident that the pristine PU showed three weight loss peaks (218°C to 360°C, 360°C to 518°C and 518°C to 745°C) and the PU/$MgCl_2$ composite showed four weight (180°C to 263°C, 263°C to 362°C, 362°C to 598°C and 598°C to 953°C) loss peaks.

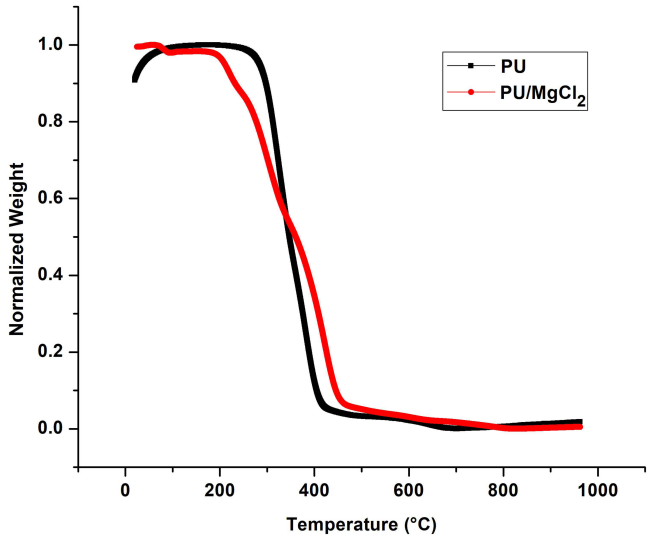

Figure 5 TGA curve of electrospun PU and PU/$MgCl_2$ patch.

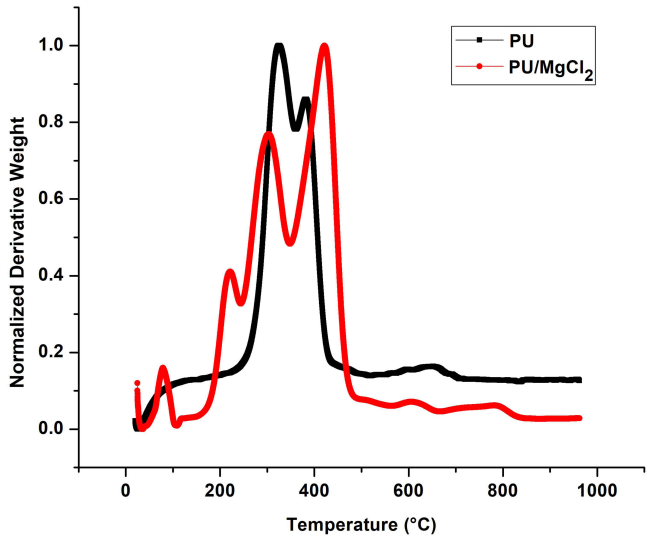

Figure 6 DTG curve of electrospun PU and PU/$MgCl_2$ patch.

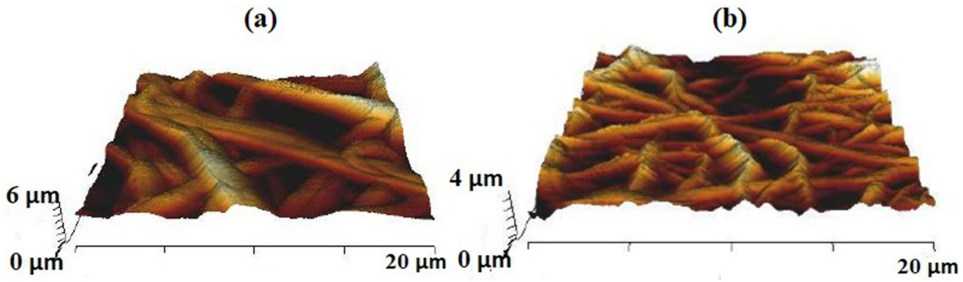

Figure 7 AFM images of (**a**) PU and (**b**) PU/ $MgCl_2$ Patch.

AFM Analysis

AFM was carried out to evaluate the surface roughness of electrospun nanofibers and their representative 3D images are shown in Figure 7. The results of the AFM analysis showed that the addition of $MgCl_2$ to the electrospun PU nanofibers led to a reduction in surface roughness. The average Root Mean Square (RMS) roughness for the PU was 854 ± 32 nm, while for the PU/ $MgCl_2$ the roughness was 419 ± 87 nm ($p < 0.05$).

Tensile Testing

Mechanical testing of the electrospun nanofibers were presented in Figure 8. A detailed examination of the mechanical properties of electrospun membranes were summarized in Table 1. It was seen that the mechanical properties of PU was increased with the addition of $MgCl_2$.

Blood Compatibility Test

The results of the blood compatibility measurements of the electrospun nanofibers showed an enhanced anticoagulant nature of the electrospun PU/ $MgCl_2$ compared to the pristine PU. Three assays were performed to evaluate the blood clotting time of the electrospun nanofibers: APTT, PT, and hemolytic assay.

The APTT assay showed that the blood clotting time of the PU/ $MgCl_2$ was 174 ± 0.5 s, while the pristine PU had a blood clotting time of 152 ± 1.2 s ($p < 0.05$). This result suggests that the presence of $MgCl_2$ in the PU matrix led to a delay in blood clotting time.

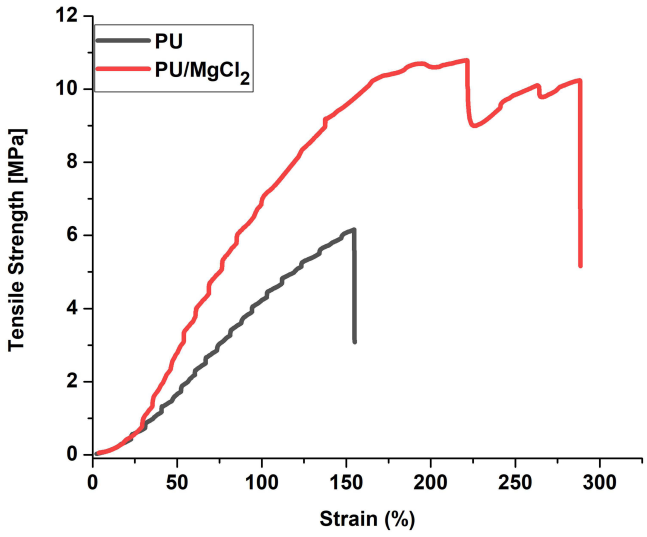

Figure 8 Tensile curves of electrospun PU and PU/$MgCl_2$ patch.

Table 1 Tensile Strength Measurements of Electrospun Membranes

Patches	Tensile strength (MPa)	Elastic modulus (MPa)	Elongation at break (%)
PU	6.66 ± 0.44	5.35 ± 0.46	69 ± 9.64
PU/$MgCl_2$	10.98 ± 0.18	8.2 ± 0.65	102 ± 11.68

The PT assay also showed a similar trend with the PU/ $MgCl_2$ having a blood clotting time of 91 ± 0.8 s, while the pristine PU had a blood clotting time of 73 ± 1.7 s ($p < 0.05$). This result further supports the observation that the addition of $MgCl_2$ to the PU matrix enhanced the anticoagulant nature of the electrospun nanofibers.

The hemolytic assay was performed to determine the toxicity of the electrospun membranes to red blood cells. The results showed that the PU/ $MgCl_2$ had a lower hemolytic index compared to the pristine PU, with a value of 1.78% compared to 2.55% ($p < 0.05$). The hemolytic index of the PU/ $MgCl_2$ was considered non-hemolytic because it was less than 2% according to ASTMF756-00(2000).[25]

In-vitro Antimicrobial Testing

The antimicrobial activity of the electrospun PU and PU/$MgCl_2$ composites were displayed in Figure 9. The zone of inhibition against the bacteria's for the electrospun PU and PU/$MgCl_2$ were evaluated after 24 hours of incubation. The pristine PU showed zero inhibition while the electrospun PU/$MgCl_2$ had greater zone of inhibition than pristine PU. According to reports, the PU membrane's showed zero zone of inhibition, whereas the electrospun PU/$MgCl_2$ showed 21.5 ± 0.5 mm (*S. Aureus*) and 27.5 ± 2.5 mm (*E. Coli*) at 500 ug/mL respectively ($p < 0.05$).

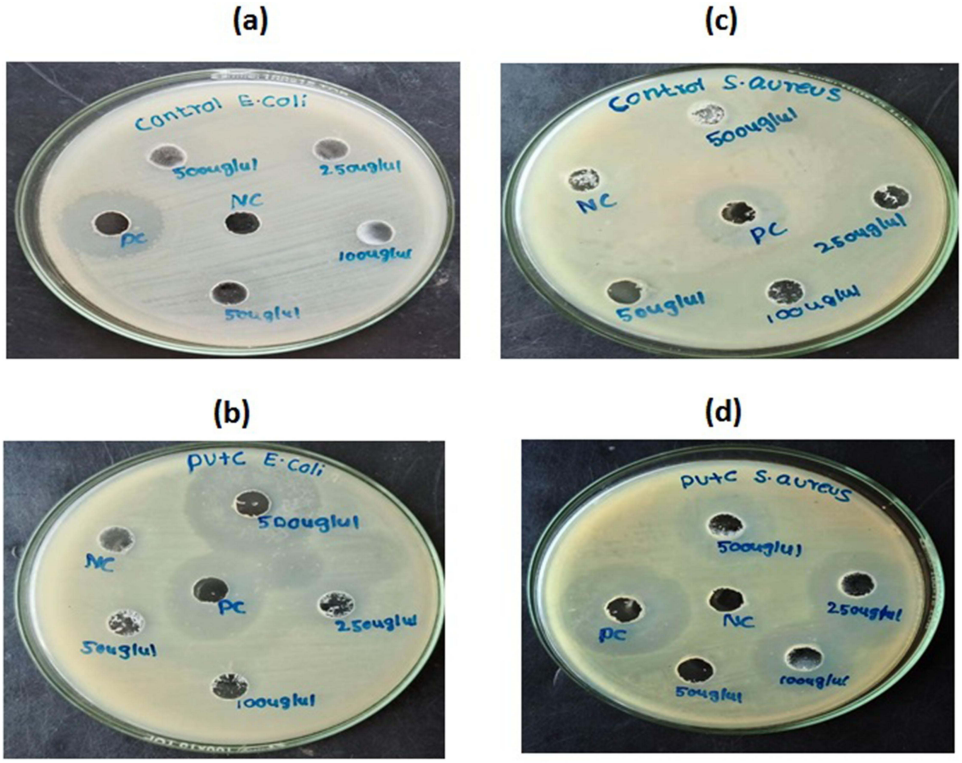

Figure 9 Zone of inhibition of (**a**) PU, (**b**) PU/$MgCl_2$ against *E. Coli* and (**c**) PU, (**d**) PU/$MgCl_2$ against *S. Aureus*..

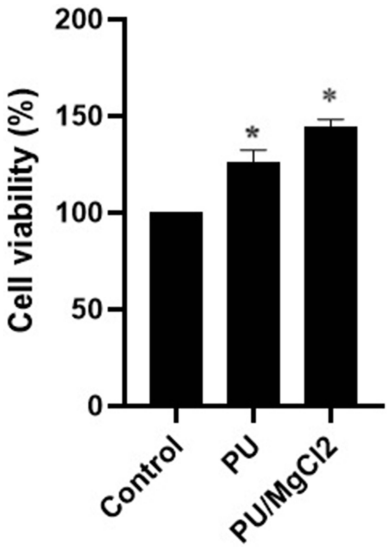

Figure 10 MTT assay of electrospun PU and PU/$MgCl_2$ patch. * denotes significance compared to control ($p<0.05$).

In-vitro Cell Viability Analysis

The fibroblast cell viability of the electrospun PU and PU/$MgCl_2$ composites is displayed in Figure 10. The fibroblast cells were adhered to the electrospun PU and PU/$MgCl_2$ after three days of cell growth. On the other hand, PU/$MgCl_2$ had greater cell viability than pristine PU. According to reports, the PU membrane's cell survival rate was 126 ± 5%, whereas the electrospun PU/$MgCl_2$ showed 145 ± 3% ($p < 0.05$).

Discussions

The results from Image J analysis showed that the addition of $MgCl_2$ decreased the fiber diameter of the pristine PU. This decrease in fiber diameter could be attributed to the increase in conductivity of the PU solution upon the addition of $MgCl_2$. Similarly, other studies have also reported that the addition of conductive agents to polymer solutions resulted in the reduction of fiber diameter. For instance, one study reported that the addition of copper sulphate ($CuSO_4$) to polyurethane resulted in the reduction of fiber diameter, which is consistent with the observation made in the present study.[22] In another research, it was reported that the addition of bioactive ursolic acid to chitosan-polyvinyl alcohol nanofiber mats resulted in smaller fiber diameter and enhanced cell viability, as compared to the control group.[26] The results of the FTIR spectra showed that the addition of $MgCl_2$ to the PU resulted in strong hydrogen bond formation and CH peak shift. Further, there is a broad peak formation due to the interaction of $MgCl_2$ with the amide group of polyurethane in the region 3318 cm^{-1} as indicated in Figure 4. In contact angle measurements, it was seen that the PU surface converts to hydrophilic on adding $MgCl_2$. This observation is supported by a previous study, where $CuSO_4$ was incorporated into polyurethane patch for wound dressing applications and found that the addition of $CuSO_4$ improved the wettability of the pristine PU.[22] The improved wettability of the PU/$MgCl_2$ nanocomposite will be favorable for wound healing applications. A hydrophilic environment is conducive for fibroblast cell adhesion and proliferation, and thus, it may lead to new tissue growth. TGA results suggests that the thermal properties of the nanocomposite were affected by the addition of $MgCl_2$. The decrease in the initial degradation temperature was due to the degradation of water molecules present in the magnesium. Further, the weight loss peak intensity increased, indicating higher weight loss, confirming the presence of $MgCl_2$ in the PU matrix as seen in the Derivative Thermogravimetric (DTG). These findings suggest that the addition of $MgCl_2$ altered the thermal stability of the PU nanocomposite. In AFM analysis, the reduction in surface roughness was attributed to the presence of $MgCl_2$. PU contains both hard and soft segments, featuring functional groups such as amino, methyl, and carboxyl groups. These functional groups are known to have the potential for ion-dipole interactions with magnesium and chlorine ions present in $MgCl_2$. Such interactions are conducive to the formation of smoother surfaces due to the alignment and bonding of these ions with the PU matrix. This phenomenon results in

a reduction in surface roughness, which is in agreement with the observed experimental data. This finding is similar to previous studies who found that the addition of $CuSO_4$ resulted in smoother surfaces in electrospun PU patch.[22] In the study by Kim et al, it was demonstrated that electrospun scaffolds fabricated using PCL exhibited smoother surfaces in smaller-diameter scaffolds compared to larger-diameter ones.[27] Our findings align with this observation, suggesting that the incorporation of $MgCl_2$ had influenced the fiber diameter. As a result, the composites developed in our study feature fibers with smaller diameters, which could contribute to the smoother surfaces observed. Furthermore, Ghorbani et al observed that the surface roughness of electrospun PU was reduced and appeared smooth after oxygen plasma modification and demonstrated improved attachment of fibroblast cells.[28] Fibroblasts play a crucial role in wound healing by producing ECM components and promoting tissue repair. Therefore, the smoother surfaces of the PU/$MgCl_2$ nanocomposites may facilitate enhanced fibroblast activity, ultimately promoting wound healing. Recent studies have underscored the significance of mechanical properties in the wound healing process.[29] Enhanced mechanical properties, such as increased tensile strength and elasticity, have been shown to positively influence various aspects of wound healing.[30] These properties can regulate the presence of myofibroblasts, microvascular blood flow, fibrosis, collagen fibril thickness, and inflammatory response. By targeting these factors, enhanced mechanical properties may aid in preventing scar formation and promoting more efficient wound healing.[31] Tensile properties findings reveal that the tensile strength, modulus, and elongation at break of PU increased notably with the addition of $MgCl_2$. These observations align with a prior study involving PU and $CuSO_4$, which reported enhanced tensile strength through the incorporation of $CuSO_4$. This enhancement in tensile strength in the PU/$MgCl_2$ nanocomposites can be attributed to the reduced fiber diameter.[22] In support of this, Wong et al documented in a separate study that patches with smaller fiber diameters exhibited improved tensile strength and modulus.[32] Consequently, the smaller diameter in our developed nanocomposite likely contributed to the enhanced tensile properties. In the blood compatibility analysis, the PU/$MgCl_2$ nanocomposites exhibited enhanced anticoagulant properties compared to pristine PU. Blood compatibility is a multifactorial phenomenon influenced by surface roughness, chemical composition, wettability, surface energy, and protein adsorption.[25] The improved anticoagulant nature of the PU/$MgCl_2$ nanocomposites can be attributed to their smaller fiber diameter, reduced surface roughness, and enhanced wettability.[33] The incorporation of $MgCl_2$ into the PU matrix resulted in a reduced fiber diameter, which likely contributed to the observed improvement in anticoagulant properties. Additionally, the smoother surface of the PU/$MgCl_2$ nanocomposites affected their wettability, making the material more hydrophilic. Our studies demonstrated that the wettability of the PU/$MgCl_2$ composites increased, which in turn positively impacted blood compatibility. These findings highlight the crucial role of wettability in determining the blood compatibility of the fabricated composites and suggest that the addition of $MgCl_2$ to electrospun PU could be a promising strategy for enhancing their performance in wound healing applications. In antimicrobial testing, PU/$MgCl_2$ nanocomposites showed enhanced activity against the gram-positive and gram-negative bacteria. Augustine et al prepared PCL scaffolds added with zinc oxide (ZnO) nanoparticles for wound dressing applications. The prepared composites displayed enhanced antimicrobial activity than the pure PCL which correlates with our findings.[34] Hence, our developed composites with enhanced antimicrobial activity might be suitable for wound re-modeling by providing an antimicrobial effect. In-vitro cell viability analysis clearly showed that cells were more viable when $MgCl_2$ was present in the pristine PU. According to published research, fibroblast cell adhesion and development will be promoted by patches with smaller fibers and hydrophilic properties.[35] As previously noted, the manufactured composites hydrophilic nature and lower fiber diameter due to $MgCl_2$ addition led to increased fibroblast cell attachment.

Conclusions

The incorporation of $MgCl_2$ into the polyurethane (PU) patches significantly enhances their mechanical properties, blood compatibility, and antimicrobial activity, which are critical factors for effective wound healing. The smooth, non-woven structure, confirmed by SEM, and strong hydrogen bond formation between PU and MgCl2, verified by FTIR, contribute to the improved tensile strength. Enhanced results in coagulation assays and reduced hemolysis indicate superior blood compatibility, while increased zones of inhibition demonstrate potent antimicrobial properties. Additionally, the MTT assay confirms the non-cytotoxic nature of the composite patches, making them promising candidates for promoting efficient wound healing.

Disclosure

The authors report no conflicts of interest in this work.

References

1. Jahromi MA, Zangabad PS, Basri SM, et al. Nanomedicine and advanced technologies for burns: preventing infection and facilitating wound healing. *Adv Drug Deliv Rev*. 2018;123:33–64. doi:10.1016/j.addr.2017.08.001
2. Jeschke MG, van Baar ME, Choudhry MA, Chung KK, Gibran NS, Logsetty S. Burn injury. *Nat Rev Dis Primers*. 2020;6(1):11. doi:10.1038/s41572-020-0145-5
3. Portela R, Leal CR, Almeida PL, Sobral RG. Bacterial cellulose: a versatile biopolymer for wound dressing applications. *Microb Biotechnol*. 2019;12(4):586–610. doi:10.1111/1751-7915.13392
4. Wendels S, Avérous L. Biobased polyurethanes for biomedical applications. *Bioact Mater*. 2021;6(4):1083–1106. doi:10.1016/j.bioactmat.2020.10.002
5. Asadi N, Del Bakhshayesh AR, Davaran S, Akbarzadeh A. Common biocompatible polymeric materials for tissue engineering and regenerative medicine. *Mater Chem Phys*. 2020;242:122528. doi:10.1016/j.matchemphys.2019.122528
6. Das A, Mahanwar P. A brief discussion on advances in polyurethane applications. *Adv Ind Eng Polym Res*. 2020;3(3):93–101. doi:10.1016/j.aiepr.2020.07.002
7. Marzec M, Kucińska-Lipka J, Kalaszczyńska I, Janik H. Development of polyurethanes for bone repair. *Mater Sci Eng C*. 2017;80:736–747. doi:10.1016/j.msec.2017.07.047
8. Afsharian YP, Rahimnejad M. Bioactive electrospun scaffolds for wound healing applications: a comprehensive review. *Polym Test*. 2021;93:106952.106952. doi:10.1016/j.polymertesting.2020.106952
9. Zhang W, Liu W, Long L, et al. Responsive multifunctional hydrogels emulating the chronic wounds healing cascade for skin repair. *J Control Release*. 2023;354:821–834. doi:10.1016/j.jconrel.2023.01.049
10. Xie X, Lei H, Fan D. Antibacterial hydrogel with pH-responsive microcarriers of slow-release VEGF for bacterial infected wounds repair. *J Mater Sci Technol*. 2023;144:198–212. doi:10.1016/j.jmst.2022.09.062
11. Brokesh AM, Gaharwar AK. Inorganic biomaterials for regenerative medicine. *ACS Appl Mater Interfaces*. 2020;12(5):5319–5344. doi:10.1021/acsami.9b17801
12. Suryavanshi A, Khanna K, Sindhu KR, Bellare J, Srivastava R. Magnesium oxide nanoparticle-loaded polycaprolactone composite electrospun fiber scaffolds for bone–soft tissue engineering applications: in-vitro and in-vivo evaluation. *Biomed Mater*. 2017;12(5):055011. doi:10.1088/1748-605X/aa792b
13. Mohanadas HP, Nair V, Doctor AA, et al. A systematic analysis of additive manufacturing techniques in the bioengineering of in vitro cardiovascular models. *Ann Biomed Eng*. 2023;51(11):2365–2383. doi:10.1007/s10439-023-03322-x
14. Keirouz A, Chung M, Kwon J, Fortunato G, Radacsi N. 2D and 3D electrospinning technologies for the fabrication of nanofibrous scaffolds for skin tissue engineering: a review. *Wiley Interdiscip Rev*. 2020;12(4):e1626. doi:10.1002/wnan.1626
15. Rahmati M, Mills DK, Urbanska AM, et al. Electrospinning for tissue engineering applications. *Procedia Mater Sci*. 2021;117:100721. doi:10.1016/j.pmatsci.2020.100721
16. Abrigo M, McArthur SL, Kingshott P. Electrospun nanofibers as dressings for chronic wound care: advances, challenges, and future prospects. *Macromol Biosci*. 2014;14(6):772–792. doi:10.1002/mabi.201300561
17. Khorshidi S, Solouk A, Mirzadeh H, et al. A review of key challenges of electrospun scaffolds for tissue-engineering applications. *J Tissue Eng Regen Med*. 2016;10(9):715–738. doi:10.1002/term.1978
18. Du W, Jiang L, Shi M, Yang Z, Zhang X. The modification mechanism and the effect of magnesium chloride on poly (vinyl alcohol) films. *RSC Adv*. 2019;9(3):1602–1612. doi:10.1039/C8RA09958H
19. Xin YZ, Quan M, Kim SS, et al. Fabrication of MgCl2/PCL composite scaffolds using 3D bio plotting system for bone regeneration. *J Biomater Tissue Eng*. 2015;5(11):849–856. doi:10.1166/jbt.2015.1374
20. Mohandas H, Sivakumar G, Kasi P, Jaganathan SK, Supriyanto E. Microwave-assisted surface modification of metallocene polyethylene for improving blood compatibility. *Biomed Res Int*. 2013;2013:1–7. doi:10.1155/2013/253473
21. Amarnath LP, Srinivas A, Ramamurthi A. In vitro hemocompatibility testing of UV-modified hyaluronan hydrogels. *Biomaterials*. 2006;27(8):1416–1424. doi:10.1016/j.biomaterials.2005.08.008
22. Jaganathan SK, Mani MP, Khudzari AZ. Electrospun combination of peppermint oil and copper sulphate with conducive physico-chemical properties for wound dressing applications. *Polymers*. 2019;11(4):586. doi:10.3390/polym11040586
23. Unnithan AR, Pichiah PT, Gnanasekaran G, et al. Emu oil-based electrospun nanofibrous scaffolds for wound skin tissue engineering. *Colloids Surf A*. 2012;415:454–460. doi:10.1016/j.colsurfa.2012.09.029
24. Tijing LD, Ruelo MT, Amarjargal A, et al. Antibacterial and superhydrophilic electrospun polyurethane nanocomposite fibers containing tourmaline nanoparticles. *Chem Eng J*. 2012;197:41–48. doi:10.1016/j.cej.2012.05.005
25. Huang N, Yang P, Leng YX, et al. Hemocompatibility of titanium oxide films. *Biomaterials*. 2003;24(13):2177–2187. doi:10.1016/S0142-9612(03)00046-2
26. Lv H, Zhao M, Li Y, et al. Electrospun chitosan–polyvinyl alcohol nanofiber dressings loaded with bioactive ursolic acid promoting diabetic wound healing. *Nanomaterials*. 2022;12(17):2933. doi:10.3390/nano12172933
27. Kim HH, Kim MJ, Ryu SJ, Ki CS, Park YH. Effect of fiber diameter on surface morphology, mechanical property, and cell behavior of electrospun poly (ε-caprolactone) mat. *Fibers Polym*. 2016;17:1033–1042. doi:10.1007/s12221-016-6350-x
28. Ghorbani F, Zamanian A, Aidun A. Conductive electrospun polyurethane-polyaniline scaffolds coated with poly (vinyl alcohol)-GPTMS under oxygen plasma surface modification. *Mater Today Commun*. 2020;22:100752. doi:10.1016/j.mtcomm.2019.100752
29. Wu K, Yang Q, Zhang L, et al. An injectable curcumin-releasing organohydrogel with non-drying property and high mechanical stability at low-temperature for expedited skin wound care. *J Mater Sci Technol*. 2023;133:123–134. doi:10.1016/j.jmst.2022.06.002

30. Chen SQ, Liao Q, Meldrum OW, et al. Mechanical properties and wound healing potential of bacterial cellulose-xyloglucan-dextran hydrogels. *Carbohydr Polym*. 2023;321:121268. doi:10.1016/j.carbpol.2023.121268
31. Barnes LA, Marshall CD, Leavitt T, et al. Mechanical forces in cutaneous wound healing: emerging therapies to minimize scar formation. *Adv Wound Care*. 2018;7(2):47–56. doi:10.1089/wound.2016.0709
32. Wong SC, Baji A, Leng S. Effect of fiber diameter on tensile properties of electrospun poly (ε-caprolactone). *Polymer*. 2008;49(21):4713–4722. doi:10.1016/j.polymer.2008.08.022
33. Mani MP, Ponnambalath Mohanadas H, Mohd Faudzi AA, et al. Preparation, design, and characterization of an electrospun polyurethane/calcium chloride nanocomposite scaffold with improved properties for skin tissue regeneration. *J Ind Text*. 2024;54:15280837241228275. doi:10.1177/15280837241228275
34. Augustine R, Malik HN, Singhal DK, et al. Electrospun polycaprolactone/ZnO nanocomposite membranes as biomaterials with antibacterial and cell adhesion properties. *J Polym Res*. 2014;21:1–7. doi:10.1007/s10965-013-0347-6
35. Zadeh KM, Luyt AS, Zarif L, et al. Electrospun polylactic acid/date palm polyphenol extract nanofibers for tissue engineering applications. *Emerg Mater*. 2019;2:141–151. doi:10.1007/s42247-019-00042-8